A 3D finite-element mesh for modeling large-scale surface deformation from subduction megathrust earthquakes: Application to Chile

H. Boulze[1], J-D. Garaud[2], E. Klein[1], L. Fleitout[1], C. Vigny[1] and V. Chiaruttini[2]

[1] Laboratoire de géologie - CNRS UMR 8538, École normale supérieure - PSL University, Paris, France

[2] DMAS, ONERA, Université Paris-Saclay, 92320, Châtillon, France

Supporting information

S1 Bathymetry of the subduction trench

To evaluate the best value for the trench depth and the trench-to-coast distance in the model, we compute the average of the bathymetry and topometry along 400 km profiles centered on the trench path (200 km eastward to the trench, 200 km westward to the trench), from the Chile Triple Junction to the north of the Arica Bend (Fig. S1-left). We use the mean value of the depth at the position of the trench (0 km in Fig. S1-right) in the model: -6000 m. For the trench-to-coast distance, we also use the mean profile to see where the iso-altitude 0 m is reached. (intersection of the blue dotted line and the red line in Fig S1-right). Along the subduction, it is on average 100 km. The methodology of this analysis using GMT (Wessel *et al.*, 2019) is based on the work of (Lemenkova, 2019).

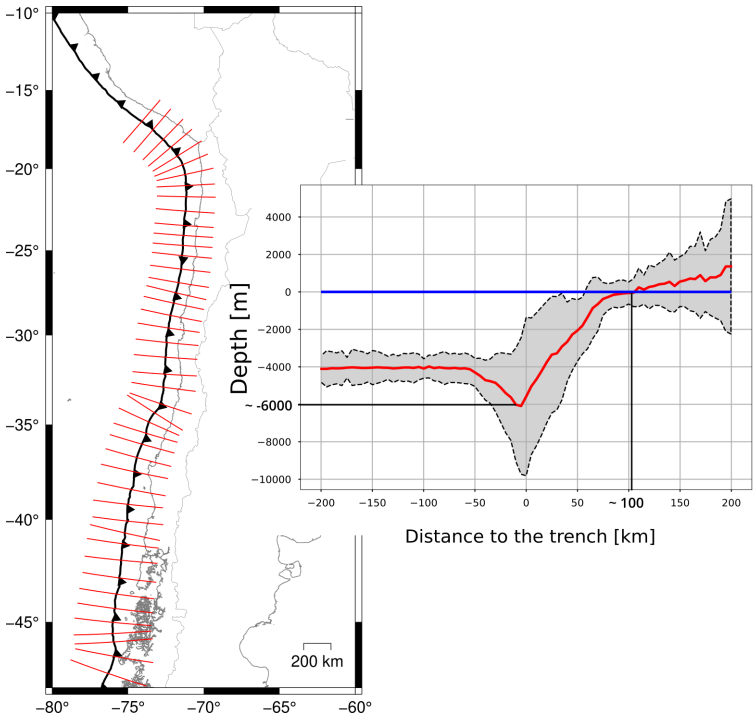

Figure S1: **Left-** The red lines depict perpendicular elevation profiles along the Chilean subduction trench. **Right-** The red line depicts the mean of the elevation profiles shown on the left figures. The gray envelope shows the amplitude of the elevation profiles along the trench. The blue line depicts altitude 0. The intersection between the 0 elevation and the mean elevation profile gives the mean distance between the fault and the coast, approximately 100 km, on average. The mean trench depth in the bathymetry is close to 6 km.

S2 Thickness of the slab and the channel

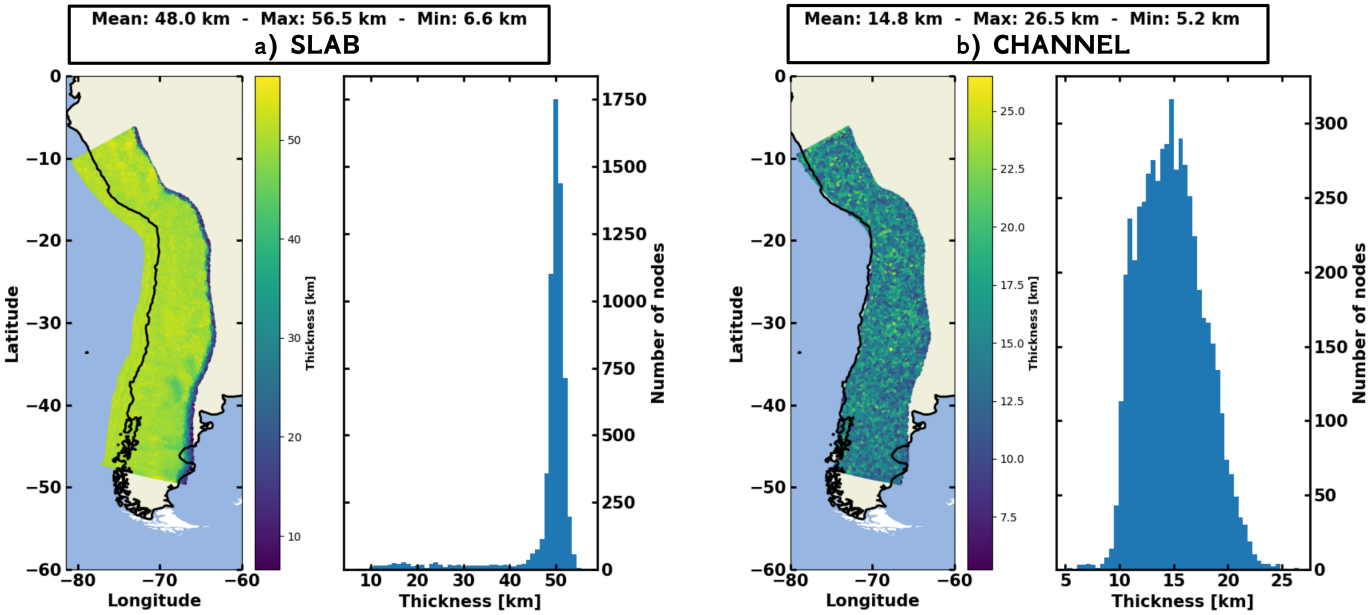

Figure S2: Thickness of the slab **(a)** and the channel **(b)** after the projection process.

S3 Coseismic slip distribution of the uniform M_w9 earthquake

We show here the coseismic slip distribution presented in Sect. 4. It is a uniform distribution of slip on the nodes of the mesh between 34° S to 38° S: all the nodes slip with an amplitude of 9 m in a direction parallel to 12° E direction.

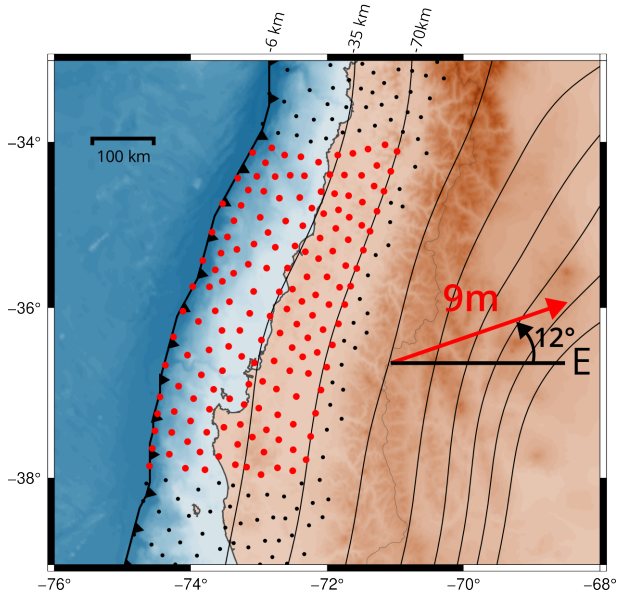

Figure S3: Coseismic slip of the fictive M_w9 earthquake. Points depict the nodes of the fault plane. Red nodes slip along a direction parallel to 12°E with a 9 m amplitude. Black nodes do not slip. Contours of Slab2.0 (Hayes *et al.*, 2018) are depicted with black lines every 35 km depth.

S4 Impact of the gravity boundary condition

We test the impact of the Earth's surface gravity boundary condition by considering two values for ρ: $\rho = 0$ (i.e. no gravity conditions) and $\rho = 3$. For the coseismic horizontal displacements, differences reach up to 10 mm at slightly over 200 km from the trench but remain below 1 % across the entire profile, indicating a negligible impact of gravity (Fig. S4a). In contrast, for the vertical displacements, differences reach more than 60 mm, corresponding to a 2 % variation. Beyond 600 km, the variations exceed 6 % and peak at 27 % at 1500 km from the trench (Fig. S4c). For the horizontal postseismic velocities at 5 yrs, differences exceed 2% within the first 250 km, peaking at approximately 0.5 mm/yr at 200 km (Fig. S4b). Beyond 400 km, variations are below 1 %. For the vertical postseismic velocities, differences average around 7 % along the entire profile, with a maximum of 2 mm/yr near the coast (Fig. S4d).

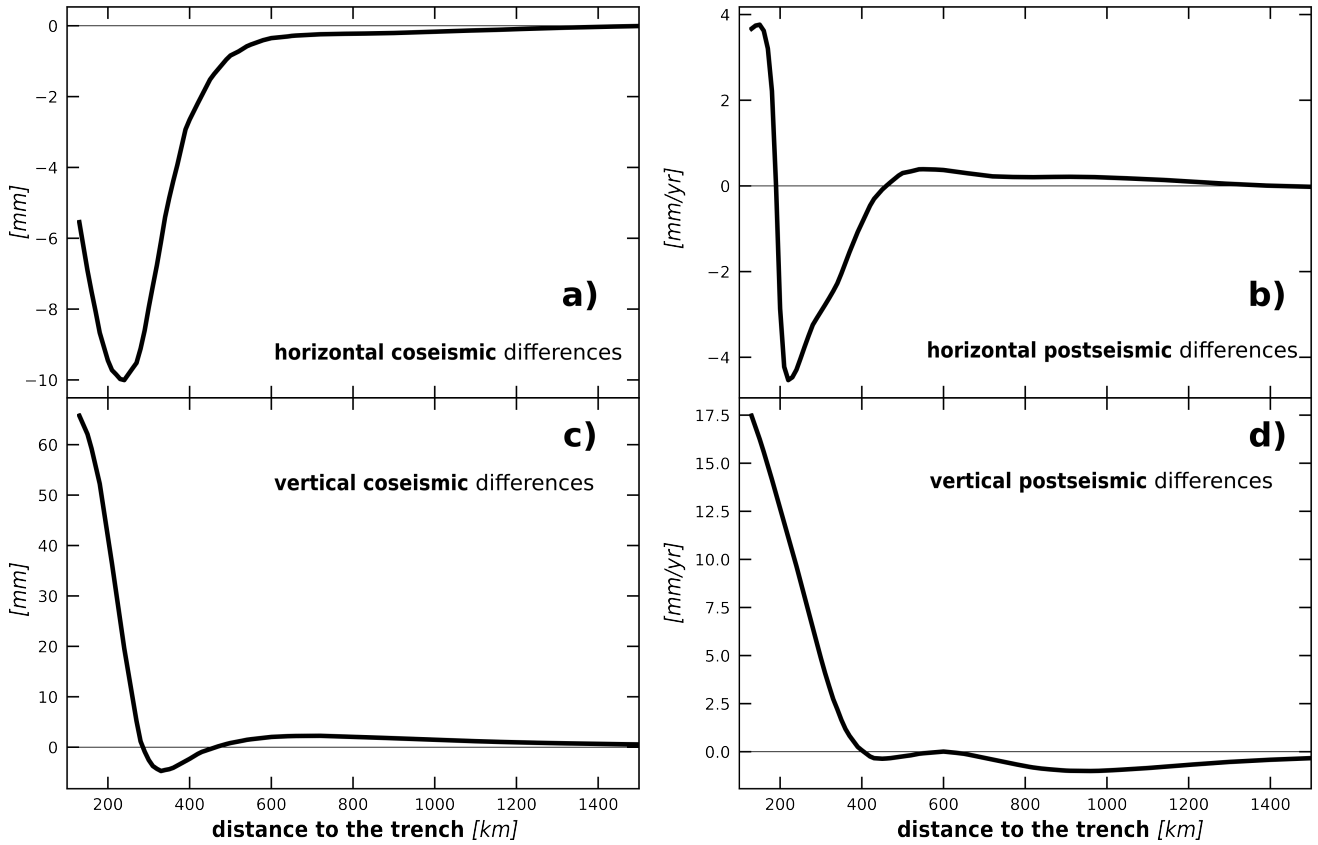

Figure S4: Differences in horizontal and vertical coseismic displacements **(a, c)** and postseismic velocities at 5 yrs **(b, d)** between models with and without a gravity boundary condition applied to the Earth's surface.

S5 Impact of the mesh depth extension

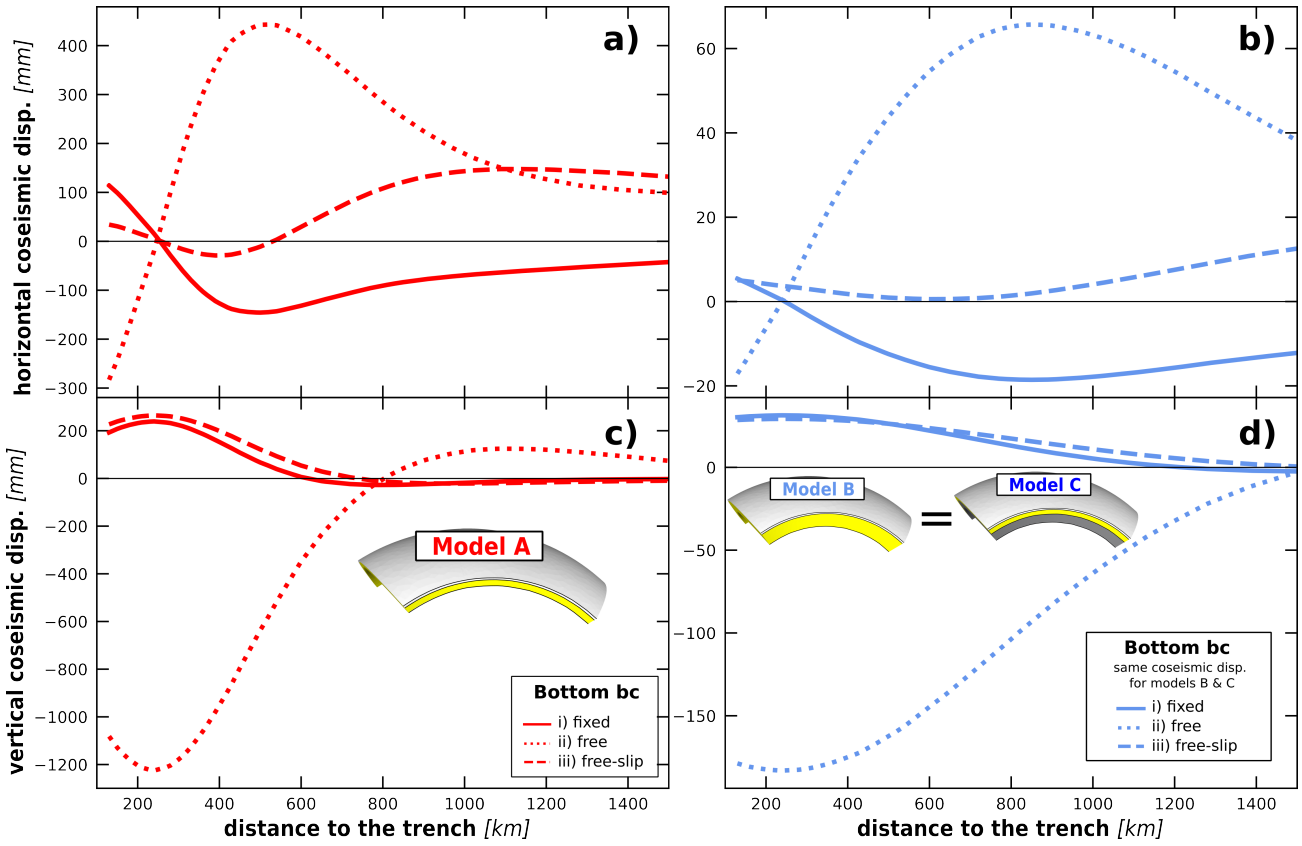

Figure S5: Horizontal **(a.)** and vertical **(c.)** differences of coseismic displacement between model A (red lines) and model R1. Horizontal **(b.)** and vertical **(d.)** difference of coseismic displacement between model B/C (blue lines) and R1. Boundary conditions at the bottom of models A and B/C vary: fixed (solid line), free (dotted line), and free-slip (dashed line). Coseismic displacements are calculated along an inland profile at 36° S (dashed orange line in Fig. 3 of the main paper).

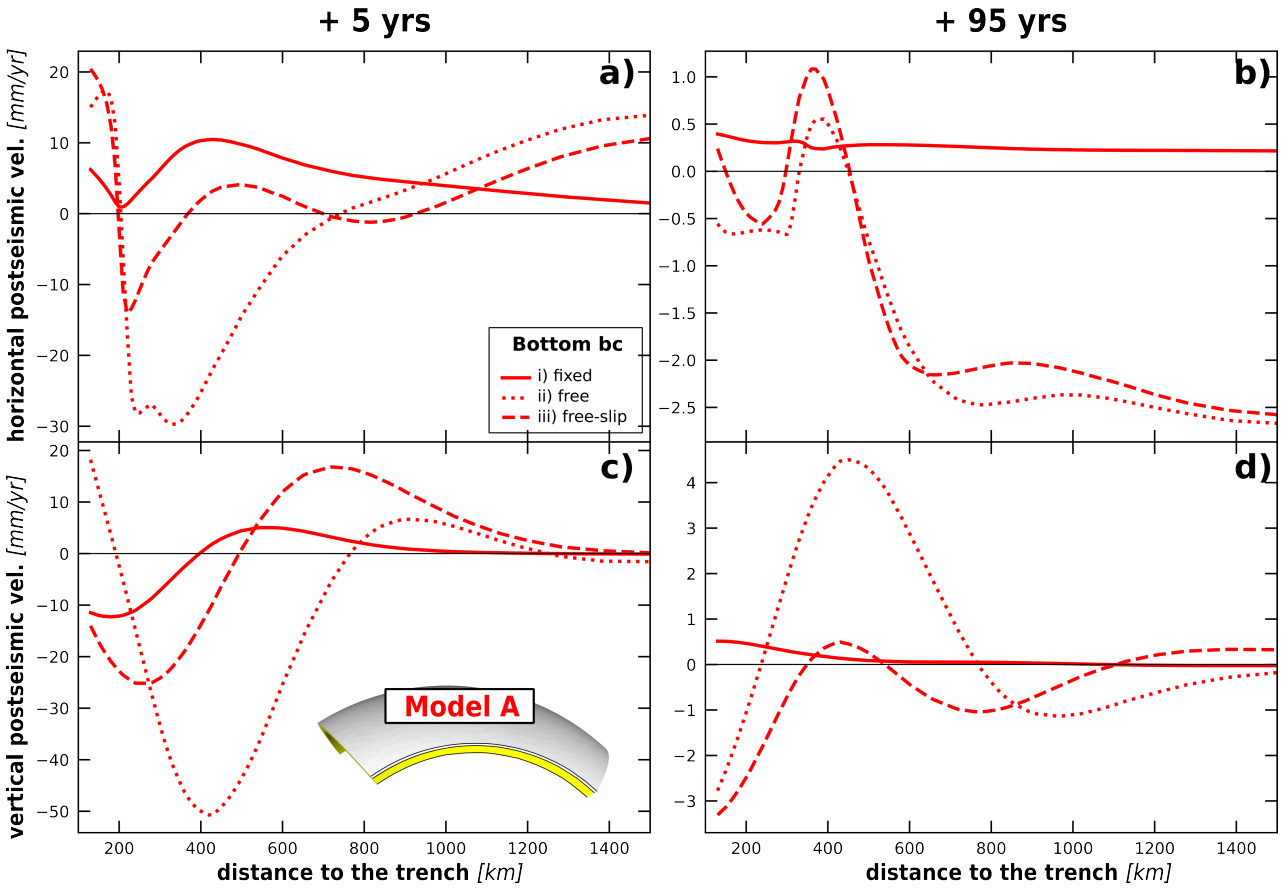

Figure S6: Horizontal **(a, b)** and vertical **(c, d)** differences of predicted postseismic velocities between predictions of model A and model R1. Panels on the left **(a, c)** show velocity differences at **+5 yrs** after the earthquake, while panels on the right **(b, d)** show velocity differences at **+95 yrs**. For model A, three different bottom boundary conditions are tested: fixed (solid red line), free (dotted red line), and free-slip (dashed red line). Postseismic velocities are calculated along an inland profile at 36° S (dashed orange line in Fig. 3 of the main paper).

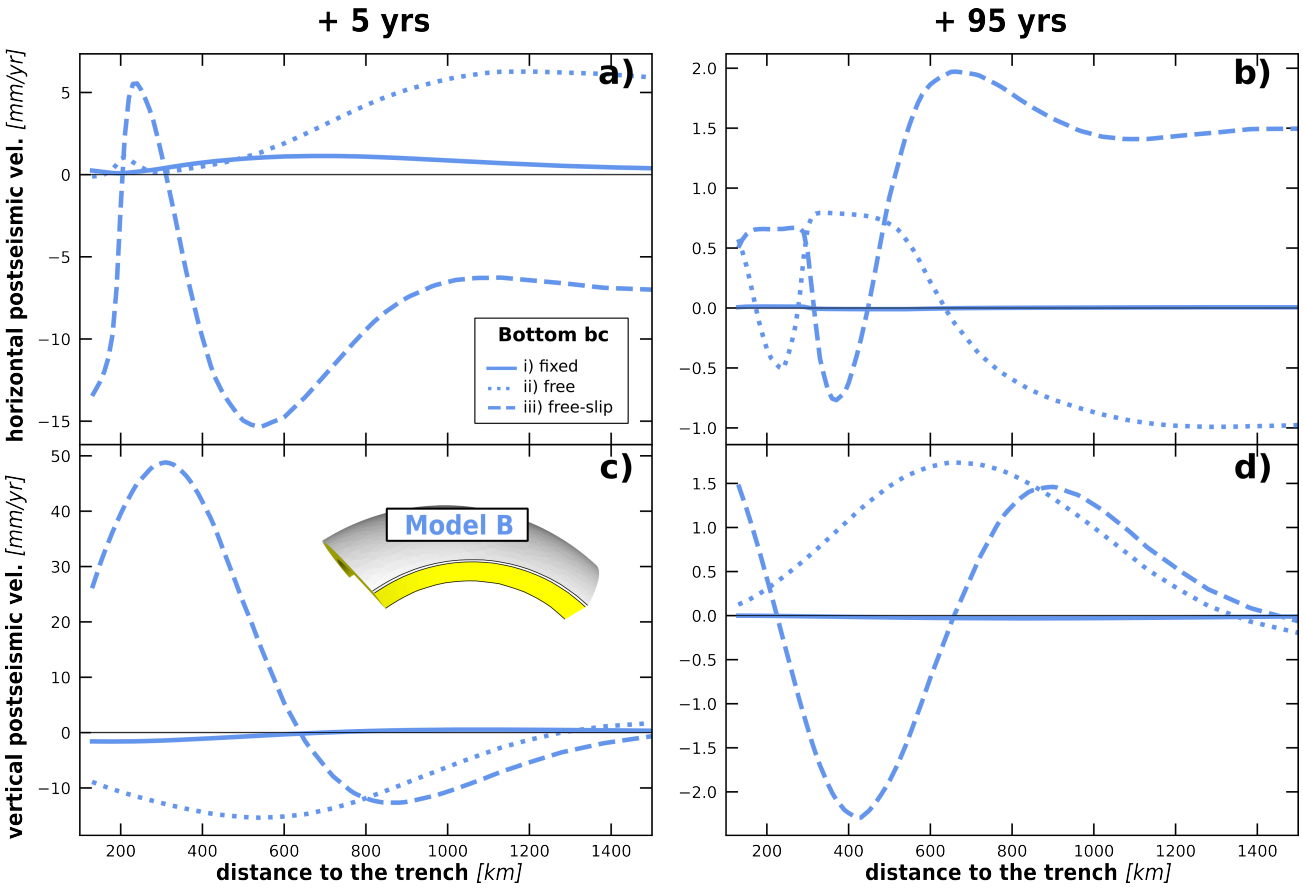

Figure S7: Same caption as Fig. S6 but for model B and R2.

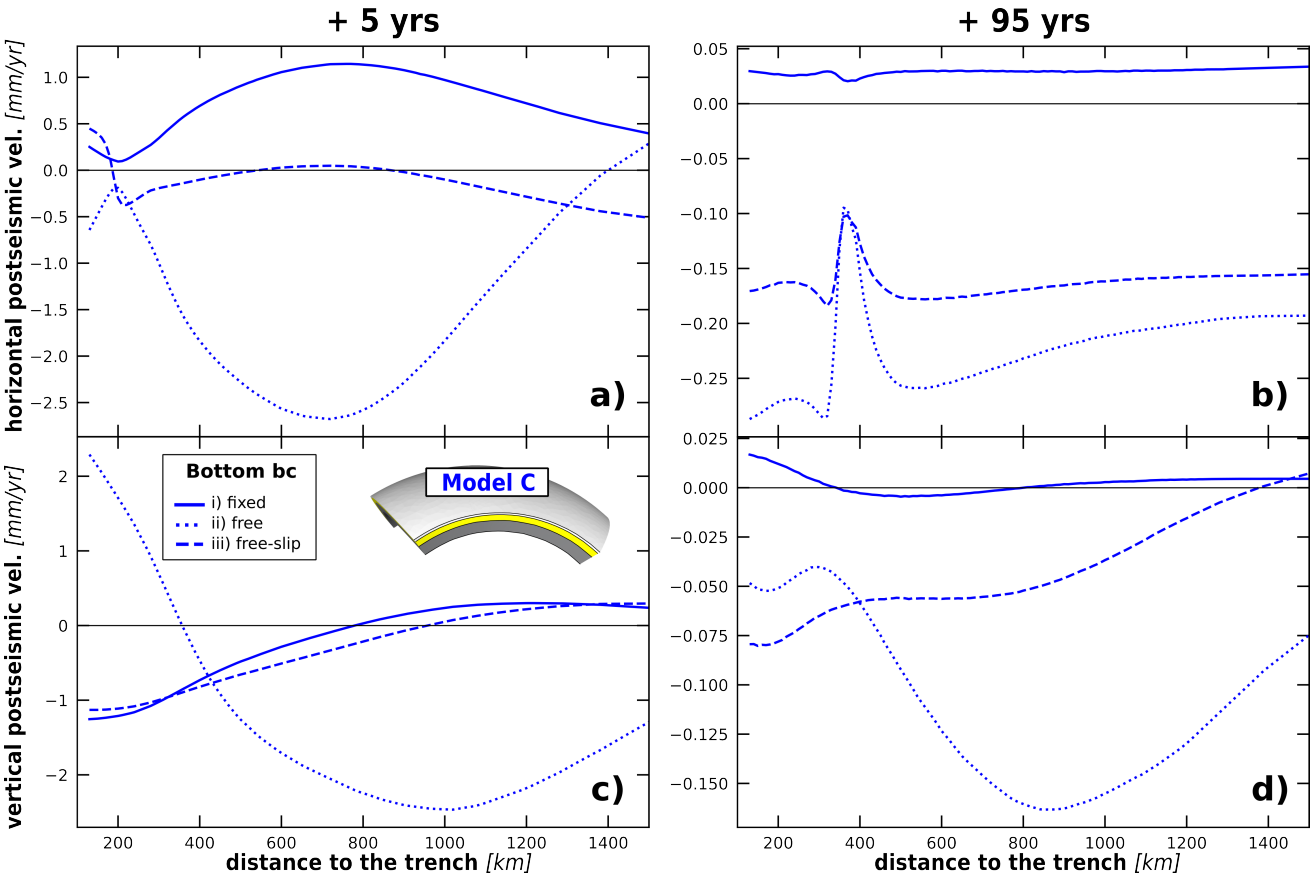

Figure S8: Same caption as Fig. S7 but for model C and R1.

S6 Impact of the mesh lateral extension

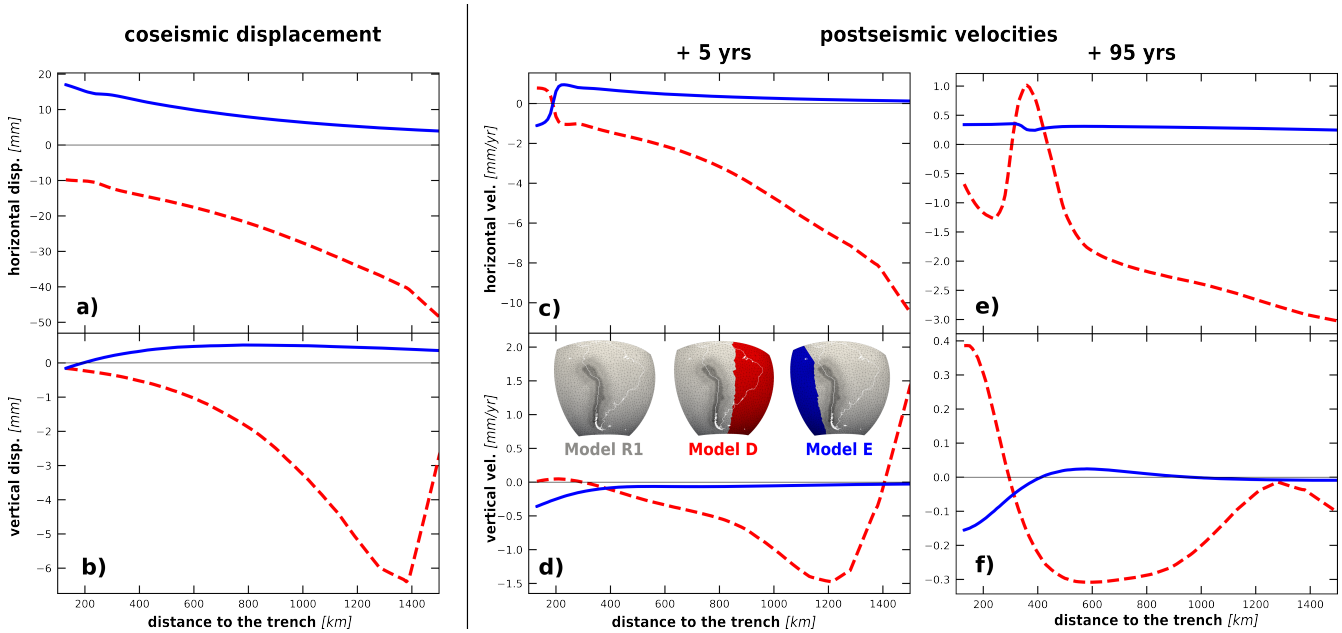

Figure S9: Horizontal **(a)** and vertical **(b)** difference of coseismic displacements between model D (red dashed line) and model E (blue solid line) with respect to model R1 (gray line). Differences in horizontal **(c, e)** and vertical **(d, f)** postseismic velocities for models D, E, and R1. Same color code for curves. Panels **(c–d)** show velocity differences at 5 yrs, and **(e–f)** at 95 yrs after the earthquake. The colored area in the insets for models D and E indicates the deactivated regions of the meshh: Only the grey area is used in the computations. Both coseismic and postseismic deformations are evaluated along an inland profile at 36°S (dashed orange line in Fig. 3 of the main paper).

S7 Variations of the slab topography

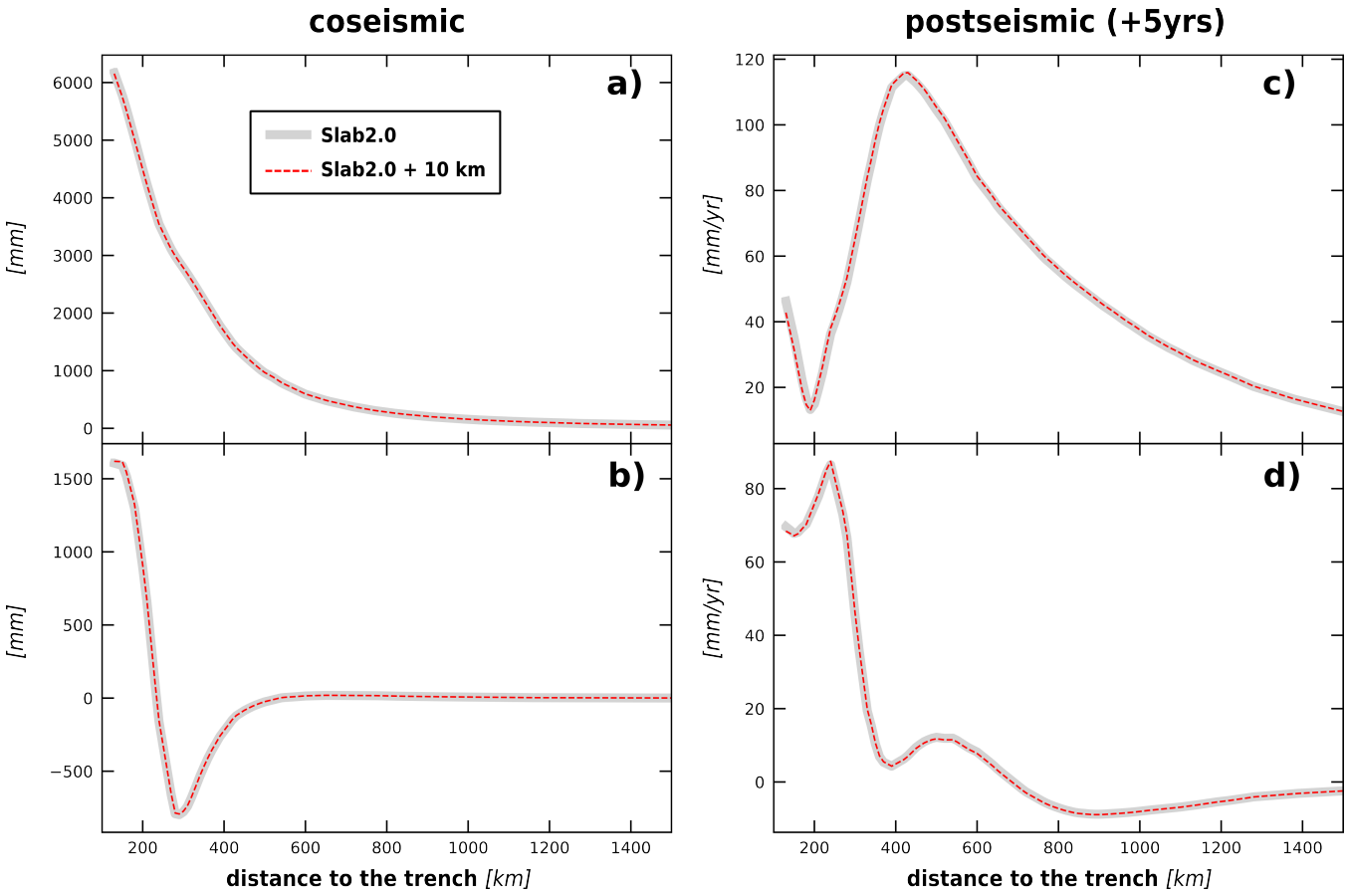

Figure S10: Horizontal **(a)** and vertical **(b)** coseismic displacements for a mesh featuring Slab2.0 (gray line) and a mesh with the Slab2.0 surface shallowed by 10 km between the trench and 40 km depth. Horizontal **(c)** and vertical **(d)** postseismic velocities at 5 yrs for the same meshes. See Table S1 for rheological parameters and Sect. 4 of the main paper for further simulation details. The same coseismic slip distribution is applied for both meshes (Fig. S3).

S8 Rheological parameters of the numerical tests

S8.1 Reference model

Table S1: Rheologies used for tests in Sect. 4 and for R1 model in Sect 5.1 and 5.2. η_M denotes the Maxwell viscosity. *See Sect. S8.3 for elastic moduli (PREM). The rheology of geophysical zones can be adjusted independently.

Geophysical zones	**Rheology**
Elastic	
Accretionary Prism Oceanic lithosphere Continental lithosphere Slab CH1	PREM*
Viscoelastic (η_M in Pa.s)	
Asthenosphere-1-Oceanic Asthenosphere-1-Continental Asthenosphere-2-Oceanic Asthenosphere-2-Continental CH2 CH3	$3 \times 10^{18} Pa.s$
Deep Upper-mantle CH4	$3 \times 10^{20} Pa.s$
Lower-mantle	$3 \times 10^{21} Pa.s$

S8.2 Impact of the depth of the mesh bounding-box

Table S2: Viscoelastic rheologies used for testing the impact of the mesh depth: models A, B, C and R2. For model R1 see Table S1. η_M denotes the Maxwell viscosity. See Sect. S8.3 for elastic moduli. Each rheology can be adjusted independently.

Geophysical zones	**Rheology**
Model A	
Viscoelastic (η_M in Pa.s)	
Asthenosphere-1-Oceanic Asthenosphere-1-Continental Asthenosphere-2-Oceanic Asthenosphere-2-Continental CH2 CH3	3×10^{18}
Model B	
Viscoelastic (η_M in Pa.s)	
Asthenosphere-1-Oceanic Asthenosphere-1-Continental Asthenosphere-2-Oceanic Asthenosphere-2-Continental CH2 CH3 CH4 Deep Upper mantle	3×10^{18}
Model C	
Viscoelastic (η_M in Pa.s)	
Asthenosphere-1-Oceanic Asthenosphere-1-Continental Asthenosphere-2-Oceanic Asthenosphere-2-Continental CH2 CH3	3×10^{18}
Deep Upper mantle	3×10^{20}
Model R2	
Viscoelastic (η_M in Pa.s)	
Asthenosphere-1-Oceanic Asthenosphere-1-Continental Asthenosphere-2-Oceanic Asthenosphere-2-Continental CH2 CH3 CH4 Deep Upper-mantle	3×10^{18}
Lower-mantle	3×10^{21}

S8.3 Elastic rheologies used for simulations

Bulk and shear moduli (in Pa) are given as functions of depth (in km). Values are based on the Preliminary Reference Earth Model (PREM) (Dziewonski et Anderson, 1981). Notice the Mohorovičić discontinuity at 30 km depth. For real simulations, differences can be implemented between continental and oceanic lithospheres.

Table S3: Shear **(G)** and Bulk **(K)** moduli for all geophysical zones. Each parameter can be adjusted independently for each geophysical zone.

G [GPa]	**K** [GPa]	**Depth** [km]
26	52	+10
Earth's surface (0 km)		
26	52	-30
68	130	-30
68	130	-60
65.6	127	-221
82.4	160	-401
90.6	176	-406
125	242	-660
155	300	-671
193	373	-1250
294	656	-2890
294	656	-3000
Core-Mantle boundary (-3000 km)		

References

Dziewonski, A. M. et Anderson, D. L. (1981). Preliminary reference earth model. *Physics of the earth and planetary interiors*, 25(4):297–356.

Hayes, G., Moore, G., Portner, D., Hearne, M., Flamme, H., Furtney, M. et Smoczyk, G. (2018). Slab2, a comprehensive subduction zone geometry model. *Science*, 362:eaat4723.

Lemenkova, P. (2019). Geomorphological modelling and mapping of the peru-chile trench by gmt. *Polish Cartographical Review*, 51(4):181–194.

Wessel, P., Luis, J. F., Uieda, L., Scharroo, R., Wobbe, F., Smith, W. H. F. et Tian, D. (2019). The Generic Mapping Tools Version 6. *Geochemistry, Geophysics, Geosystems*, 20(11):5556–5564. _eprint: https://agupubs.onlinelibrary.wiley.com/doi/pdf/10.1029/2019GC008515.